Theory of the excitonic effect in solid C_{60}

Xudong Jiang and Zizhao Gan

Department of Physics and National Laboratory of Mesoscopic Physics, Peking University, Beijing 100871, China

(Received 10 March 1995; revised manuscript received 12 June 1995)

In this paper a theory of the excitonic effect in solid C_{60} is presented. We first develop an empirical pseudopotential method to calculate the energy levels of the C_{60} molecule, which provides a good basis for the inspection of optical transitions in both the C_{60} molecule and solid C_{60}. Then a theory is established to describe the characters of excitons in solid C_{60}. It is found that excitons in solid C_{60} are intermediates between the Frenkel and Wannier types and the photoabsorptions in solid C_{60} are mainly due to the excitonic transitions. The dielectric function of solid C_{60} is calculated based on this theory and some relevant experimental results are discussed.

I. INTRODUCTION

There have been many reports on the absorption spectra and photoconductivity of solid C_{60}.[1-3] The absorption spectrum of solid C_{60} is similar to that of the C_{60} molecule,[4-6] only with a redshift and broadening in each peak of solid C_{60} with respect to that of the C_{60} molecule. The long-wavelength limits of both photoabsorption and photoconductivity lie between 1.5 and 1.8 eV. The explanation of absorption spectra and photoconductivity in solid C_{60} remains unresolved.

Some band-structure calculations from first principles using the local-density approximation (LDA) to the density-functional theory (DFT) have been performed.[7-9] Solid C_{60} is a narrow-band insulator, with a direct gap at X. The calculated energy gap lies between 1.18 and 1.5 eV. Several authors[1-3] attributed the optical transitions and photoconductivity in solid C_{60} to interband transitions. Other authors[10-14] thought that solid C_{60} is essentially a molecular crystal and optical transitions in it should be attributed to excitonic transitions. But, as pointed out by Resca,[15] there has not been a precise theoretical description of the excitonic structure in solid C_{60}. Recent photoemission (PE) and inverse photoemission (IPE) experiments revealed that the band gap of solid C_{60} lies between 2.3 and 2.7 eV,[13,16-18] which is much larger than those obtained from the energy-band calculation of the LDA and the long-wavelength limits of optical absorption and photoconductivity. Theoretically, LDA calculations usually underestimate the energy gap of a system. Recently, Shirley and Louie[19] used a quasiparticle approach to calculate the band structure of solid C_{60}. Due to the inclusion of many-body corrections, it is usually believed that this method will give the correct value of energy gap E_g.[20] The energy gap obtained in Ref. 19 is 2.2 eV, which is much larger than that obtained from the LDA, in good agreement with experiments.

According to us, solid C_{60} is fundamentally a molecular crystal bound by van der Waals forces. The intermolecular hopping matrix elements for an electron or a hole are rather small and the Coulomb correlation energy between a pair of electrons (or electron-hole, hole-hole) are

larger than energy bandwidths. Therefore, photoabsorptions in solid C_{60} should be due to excitonic excitations. In a typical molecular crystal, an exciton is an excited state of a single molecule.[21] The propagation of an exciton is merely the propagation of a molecular excited state. Such an exciton is called a Frenkel exciton. But there are some differences in solid C_{60}. As will be pointed out later, though an exciton in solid C_{60} is mainly the excited state of the C_{60} molecule (Frenkel exciton), it contains a considerable component of the state of $C_{60}{}^{+}$-$C_{60}{}^{-}$ (i.e., the state in which electron and hole stay on different molecules). That is to say, excitons in solid C_{60} are mixed states of both Frenkel and Wannier excitons. A complete explanation of photoabsorption and photoconductivity in solid C_{60} should be given under such a picture. The present paper provides a theoretical analysis of excitonic states and optical transitions in solid C_{60}.

In Sec. II we present a description of the electronic structure in the C_{60} molecule and a discussion of the corresponding optical transitions. In Sec. III we discuss the excitonic states in solid C_{60}. In Sec. IV an approximate method is introduced to concretely calculate excitonic states in solid C_{60}. Section V provides a theoretical analysis of optical transitions in solid C_{60}. Conclusions are drawn in Sec. VI.

II. ELECTRONIC STRUCTURE AND OPTICAL TRANSITIONS IN THE C_{60} MOLECULE

Much research work has been done to investigate the electronic states in the C_{60} molecule.[7,22] For the convenience of discussing electronic structure, optical, and transport properties in solid C_{60}, the authors of this paper develop a method to describe the electronic states in the C_{60} molecule. Such a method is in fact an empirical pseudopotential method (EPM) which is in close analogy to the EPM used in the calculation of the energy-band structure of solids.[23] The details of this method and its application to the description of optical and transport properties of solid C_{60} will be presented elsewhere.[24] Here we just give a concise description.

     <u>52</u>   14 254

In the calculation of the energy-band structure of solids using the EPM, the first step is to compose the smooth part of an electron's wave function with some plane waves, i.e., adopting the empty lattice approximation. Correspondingly, in the calculation of the C$_{60}$ molecule's electronic structure, the first step is to take the approximation of a spherically symmetric well, as Troullier and Martins have done.[9] The bottom of this well occurs on a spherical surface with a radius of $\sim$ 3.55 Å and a width of $\sim$ 3.0 Å. The wave functions are the product of a radical $R_l(r)$ with a spherical harmonic Y_{lm}, where l is the angular momentum. $R_l(r)$ satisfies

$$\left[-\frac{\hbar^2}{2m}\frac{d^2}{dr^2} + \frac{\hbar^2}{2m}\frac{l(l+1)}{r^2} + V_0(r)\right](rR_l) = \varepsilon_l(rR_l) , \quad (1)$$

where $V_0(r)$ represents the spherically symmetric potential experienced by a π electron. When the I_h symmetry is introduced into this potential well, the electronic states can be described in terms of molecular symmetry-adapted functions $\chi^l(\alpha, s, n)$:

$$\chi^l(\alpha, s, n) = \sum_m \eta(l, \alpha, s, n|m)Y_{lm} , \quad (2)$$

where (α, s, n) labels the irreducible representation α of the icosahedral point group I_h, s distinguishing between representations that occur more than once. Under the same l, n denotes the rows of a given representation. The wave functions $R_l(r)\chi^l(\alpha, s, n)$ correspond to the plane waves used in the empty lattice approximation and are zeroth order approximations to the smooth part of the π electrons' wave functions. We introduce the pseudopotential V_p which belongs to the identity representation A_g of the I_h group and can be written as

$$V_p = \sum_{L\neq0} V_L(r)\chi^L(A_g, s, 1) . \quad (3)$$

From the theory of the representation of the I_h group, it is found that $L = 6, 10, 12, 14, \ldots$. The term with $L = 0$ is V_0, which has been taken into account in Eq. (1).

For the convenience of calculation, we further assume that

$$\varepsilon_l \approx \varepsilon_0 + \frac{\hbar^2}{2m}\frac{l(l+1)}{R^2} , \quad (4)$$
$$R_l \approx R_0 .$$

The zeroth wave functions under the empty lattice approximation become $R_0(r)\chi^l(\alpha, s, n)$. Taking V_p as the Hamiltonian for the next step approximation, one gets the secular equation

$$\det|(\varepsilon_\alpha - \varepsilon_l)\delta_{ll'} + \bar{v}_p(l, l', \alpha)| = 0 . \quad (5)$$

The solutions of this equation are the energies of individual energy levels (l, α), where

$$\bar{v}_p(l, l', \alpha)$$
$$= \sum_L C_L\langle\chi^l(\alpha, s, n)|\chi^L(A_g, \tilde{s}, 1)|\chi^{l'}(\alpha, s', n)\rangle ,$$
$$C_L = \int V_L(r)|R_0(r)|^2 r^2 dr . \quad (6)$$

C_L are parameters for the empirical pseudopotential, which can be determined through the comparison of energy levels obtained here to some experimental features of the photoabsorption spectrum or some other theoretical results. We fitted our parameters to the energy levels obtained from the LDA by Saito and Oshiyama.[7] The separation between the highest occupied molecular orbital (HOMO) and lowest unoccupied molecular oribital (LUMO) obtained in Ref. 7 is 1.9 eV and the excitation energy of the transition $h_u \to t_{1g}$ is 2.9 eV. From the conditions $E_{\text{LUMO}} - E_{\text{HOMO}} = 1.9$ eV and $E_{\text{LUMO+1}} - E_{\text{HOMO}} = 2.9$ eV, we got $C_6 = -9.12$ eV and $C_{10} = 17.52$ eV. With such a selection of parameters, we obtained the electronic energy levels of the C$_{60}$ molecule, which are in good agreement with those obtained from first-principle calculations. The excitation energies for the lowest optically allowed transitions $h_u \to t_{1g}$, $h_g \to t_{1u}$, and $h_u \to h_g$ are 2.9, 3.2, and 4.2 eV obtained from our calculation. These values compare well with the LDA values of 2.9, 3.1, and 4.2 eV.[7] Several levels near the HOMO and LUMO are shown in Fig. 1. It is immediately possible to determine the dipole-transition selection rules from symmetry, as indicated in this figure.

The energy difference between two adjacent spherical levels is $\Delta\varepsilon_l = \varepsilon_{l+1} - \varepsilon_l \sim 0.605(l+1)$ eV and will increase with increasing l. V_p is the sum of the ordinary potential of the core and the repulsive potential generated from the orthogonalization of the state of the π electrons with that of inner and σ electrons and is rather weak. It is expected that each level in the C$_{60}$ molecule will possess a dominant angular momentum and will have little mixture with other spherical levels with different l's. Our calculation confirms this and Troullier and Martins also found this from their calculation.[9] The dominant angular momentum l of each state is given in Fig. 1, and are in accordance with the results obtained by Troullier and Martins (see Table III in Ref. 9).

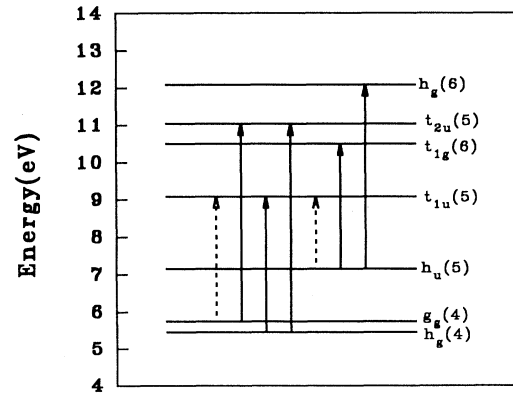It is worthwhile to point out that such a method can

FIG. 1. Several energy levels near the HOMO and LUMO of the C$_{60}$ molecule within the EPM. These levels are labeled in terms of irreducible representations of the I_h group. Also listed in parentheses are the dominant angular momentum l of each state. Solid and dashed lines represent dipole-allowed and dipole-forbidden transitions between two energy levels.

be directly generalized to calculate the energy levels of the $C_{60}{}^{n\pm}$ molecules. In the calculations of energy levels of the $C_{60}{}^{n\pm}$ molecules from *ab initio* schemes, the geometries of these molecules are fixed at that of the C_{60} molecule, i.e., neglecting the relaxation of the charge density when electrons are added to or removed from the C_{60} molecule.[25,26] Under such a situation, one can also obtain a set of spherical energy levels at first and then introduce the pseudopotential which possesses the symmetry of the molecule to split those spherical levels. By fitting to a first-principles molecular calculation, several parameters involved in the pseudopotential can be determined. We focus on the optical transitions in the C_{60} molecule and hence it is not necessary to calculate the energy levels of the $C_{60}{}^{n\pm}$ molecules here.

There is close similarity between the method we developed here and that developed by Gallup.[27] In his method, Gallup used the free electron model (FEM) to obtain the electronic structure of π electrons under spherical symmetry and then used zero-range potentials (ZRP's) to reduce the symmetry to icosahedral. The ZRP in his method plays the same role as V_p used in our calculation. Another similar method has been adopted by Saito *et al.*,[28] who divided the one-electron Hamiltonian into a spherical term H_0 and an icosahedral perturbation H_{I_h}. H_{I_h} is expanded in terms of the I_h-invariant, irreducible tensor form of sixth and tenth rank.[29] There are also several parameters involved in their calculation and by selecting fitting parameters a set of energy levels of the C_{60} molecule can be obtained.

Much experimental work has been performed on the absorption spectra of the C_{60} molecule.[4–6] In general, there are three strong peaks centered at 3.8, 4.8, and 5.9 eV. Also there is a weak peak centered at ~ 3.0 eV. The assignments of these absorption bands will be given in Sec. V.

It is not adequate to analyze optical transitions in the C_{60} molecule merely based on the energy levels shown in Fig. 1. Two other interactions should be taken into account: (i) the configurational splitting which is due to the role of the fraction of electron-electron interaction which cannot be attributed to the single electron's central force field; (ii) the coupling between molecular vibrations and electronic states, i.e., the Jahn-Teller effect.[30] Both the configurational splitting and Jahn-Teller effect will cause the splitting of a degenerate excited state. In photoabsorption, there is another kind of transition, associated with the excitation of vibrational levels.[31,32] In the EPM framework, these issues can be discussed in terms of clear physical pictures, but this will not be done in detail here.

III. EXCITONS IN SOLID C_{60}

As mentioned in Sec. I, solid C_{60} is a molecular crystal bound basically by van der Waals forces. Conduction bands in solid C_{60} can be considered to describe the propagation of the state of $C_{60}{}^{-}$ and valence bands the propagation of the state of $C_{60}{}^{+}$. With the notation of electronic states in the C_{60} molecule described in Sec. II, the Hamiltonian for electrons (or holes) in solid C_{60} can

be written as

$$H = \sum_i \sum_{\alpha,n} \varepsilon_\alpha A^\dagger_{i\alpha n} A_{i\alpha n}$$

$$+ \sum_i \sum_{\alpha,n} \sum_{\alpha',n'} (V_{i,\alpha n\alpha'n'} A^\dagger_{i\alpha n} A_{i\alpha'n'} + \text{H.c.})$$

$$+ \sum_i \sum_{j\neq i} \sum_{\alpha,n} \sum_{\alpha',n'} (\lambda_{i,\alpha n\alpha'n'} A^\dagger_{i\alpha n} A_{j\alpha'n'} + \text{H.c.}) \ . \quad (7)$$

Here (α, n) denote the single-electron states of the C_{60} molecule. For simplicity, α is used instead of (l, α, s) in Sec. II, while i, j label lattice sites. $A^\dagger_{i\alpha n}$ and $A_{i\alpha n}$ are the quantum creation and annihilation operators of electrons on site i, respectively. The second term in Eq. (7) is the interaction due to the crystal field, i.e., the interaction on single-electron levels of $C_{60}{}^{-}$ (or single-hole levels of $C_{60}{}^{+}$) at site i induced by other molecules. The third term in Eq. (7) describes the hopping of electrons (or holes) between different sites. It should be pointed out that the symmetry of the solid C_{60} lattice is always lower than that of the C_{60} molecule. The second term in Eq. (7) reflects the symmetry of the surroundings of site i, and, approximately, it reflects the symmetry of the nearest neighbors of molecule i. In principle, one can diagonalize the first and second terms in Eq. (7) to get new states $(\tilde\alpha, \tilde n)$, which possess the point group symmetry of site i. Such a symmetry is lower than I_h symmetry. Then some former levels will split. Under these new states $(\tilde\alpha, \tilde n)$, the third term in Eq. (7) will have the form of $\lambda_{i,\tilde\alpha\tilde n\tilde\alpha'\tilde n'}$. In this paper, we will not discuss such details. In the following, we will not discriminate in general between the use of $(\tilde\alpha, \tilde n)$ and (α, n).

Introducing creation and annihilation operators for holes,

$$B^\dagger_{i\beta m} = A_{i\beta m} \ , \\ B_{i\beta m} = A^\dagger_{i\beta m} \ , \quad (8)$$

with respect to the ground state, the energy of an electron-hole pair $A^\dagger_{i\alpha n} B^\dagger_{j\beta m} |0\rangle$ is

$$\varepsilon_{\alpha,\beta} = \varepsilon_\alpha - \varepsilon_\beta + W(i,j), \quad (9)$$

where

$$W(i,j) = \begin{cases} -U & \text{if } i = j \\ W(i-j) & \text{if } i \neq j. \end{cases} \quad (10)$$

Here, U is the on-site Coulomb interaction between an electron-hole pair. $W(i-j)$ is the Coulomb interaction between a $C_{60}{}^{+}$ and a $C_{60}{}^{-}$ molecule situated at sites i and j, respectively. Approximately, $W(i-j)$ is

$$W(i-j) = -\frac{e^2}{\varepsilon R_{ij}} \ , \quad (11)$$

where ε is the dielectric constant of solid C_{60} and R_{ij} is the distance between two molecular centers. In Bloch representation, the Hamiltonian for an electron-hole pair is

$$H = \sum_{\mathbf{k}_1} \sum_{\alpha,n} \varepsilon_e(\alpha n, \mathbf{k}_1) A^\dagger(\alpha n, \mathbf{k}_1) A(\alpha n, \mathbf{k}_1) + \sum_{\mathbf{k}_2} \sum_{\beta,m} \varepsilon_h(\beta m, \mathbf{k}_2) B^\dagger(\beta m, \mathbf{k}_2) B(\beta m, \mathbf{k}_2)$$

$$+ \sum_{\mathbf{k}_1} \sum_{\mathbf{k}_2} \sum_{\mathbf{q}} \sum_{\alpha,n} \sum_{\beta,m} W_{\alpha n,\beta m}(\mathbf{q}) A^\dagger(\alpha n, \mathbf{k}_1 + \mathbf{q}) B^\dagger(\beta m, \mathbf{k}_2 - \mathbf{q}) B(\beta m, \mathbf{k}_2) A(\alpha n, \mathbf{k}_1) . \tag{12}$$

The relation between energy bands of holes and electrons is

$$\varepsilon_h(\beta m, \mathbf{k}) = -\varepsilon_e(\beta m, -\mathbf{k}) \tag{13}$$

and $W(\mathbf{q})$ is the lattice Fourier transformation of $W(i,j)$.

According to theoretical calculations, the energy bands near the forbidden gap in solid C$_{60}$ are rather narrow. The bandwidths of these energy bands are about 1 eV. As for the Coulomb correlation energy U, several experimental and theoretical estimates have been provided,[13,25,26,33] in the range of 1.5–2 eV. The dielectric constant of solid C$_{60}$ is ~ 4;[34] hence $W(i-j)$ is always less than 0.3 eV and decreases rapidly with increasing R_{ij}. Therefore the problem of the exciton in solid C$_{60}$ is analogous to that of a very "heavy" particle moving in a potential well with a rather deep center. To semiquantitatively analyze this problem, from now on we will take the following approximation:

$$W(i,j) = \begin{cases} -U & \text{if } i = j \\ 0 & \text{if } i \neq j. \end{cases} \tag{14}$$

We will discuss the discrete and continuous spectra of excitons in solid C$_{60}$ under such an approximation, and correspondingly discuss the photoabsorption and photoconductivity. Before doing so, we will briefly refer to another kind of excitonic effect in solid C$_{60}$. Let us consider the interaction of electrons between different molecules. In terms of quantum operators of electrons and holes in the C$_{60}$ molecule, there will be the following terms:

$$A^\dagger_{i\alpha n} B^\dagger_{i\beta m} B_{j\beta'm'} A_{j\alpha'n'} . \tag{15}$$

These terms essentially represent a kind of dipole-dipole interaction, which means that the annihilation of an e-h pair in C$_{60}$* (an excited C$_{60}$ molecule) situated at site j will induce the excitation of the C$_{60}$ molecule situated at site i. Such interaction will also induce the propagation of C$_{60}$* in solid C$_{60}$. The interactions in Eq. (15) are proportional to $1/R_{ij}^3$ and are rather small. In this paper we will not discuss them further. As is well known, this kind of interaction is very important in the problems of excitons in typical molecular crystals.[21]

IV. A MODEL FOR CALCULATION OF EXCITONIC STATES IN SOLID C$_{60}$

As just mentioned above, the optically produced exciton in solid C$_{60}$ can be regarded as a particle with kinetic energy $\varepsilon_{ex}(\mathbf{k}) \approx \varepsilon_e(\mathbf{k}) + \varepsilon_h(-\mathbf{k})$ moving in the potential (14). Such a problem corresponds to the Koster-Slater model of impurity states in solids.[35,36] If $\varepsilon_{ex}(\mathbf{k})$ is taken to be the eigenenergy of an equivalent tight-binding

Hamiltonian (TBH), one can define the single-particle Green's function of a lattice

$$G_0(z) = \sum_{l,m} G_0(l, m, z) a_l^\dagger a_m ,$$

$$G_0(l, m, z) = \frac{1}{N} \sum_{\mathbf{k}} \frac{1}{z - \varepsilon_{ex}(\mathbf{k})} e^{[i\mathbf{k}\cdot(\mathbf{R}_l - \mathbf{R}_m)]} . \tag{16}$$

The "impurity" potential is

$$H_1 = -U a_0^\dagger a_0 . \tag{17}$$

Here, a_i and $a_i^\dagger$ are the equivalent quantum annihilation and creation operators in the TBH, respectively, l, m label the lattice sites, and $\mathbf{R}_l$, $\mathbf{R}_m$ are the corresponding lattice vectors. Equation (17) is evidently a reformulation of Eq. (14).

The Green's function of a crystal lattice with an impurity potential is

$$G = G_0 + G_0 T G_0 . \tag{18}$$

The t matrix T is

$$T = -\frac{U}{1 + U G_0(0, 0, z)} a_0^\dagger a_0 . \tag{19}$$

The condition for the occurrence of bound states (discrete spectrum) is

$$1 + U G_0(0, 0, z) = 0 . \tag{20}$$

The corresponding wave function of a bound state with $z = E_B$ is

$$|\psi_{E_B}\rangle = \sum_i b_{B,i} a_i^\dagger |0\rangle_i , \tag{21}$$

where

$$b_{B,i} = \frac{G_0(i, 0, E_B)}{\sqrt{-G_0'(0, 0, E_B)}} . \tag{22}$$

The wave functions of continuous spectra can also be obtained from Eqs. (18) and (19). The problem is thus transformed into seeking $\varepsilon_{ex}(\mathbf{k})$ and calculating G_0.

But in solid C$_{60}$ the C$_{60}$ molecule at a certain site actually has orientational disorder, even at low temperature.[37] If we view the electronic states of Eq. (7) as referring to the local coordinate system of a C$_{60}$ molecule, these local coordinate systems on individual lattice sites are in fact stochastic. The matrix elements involved in the second and third terms of Eq. (7) become random quantities, and the Hamiltonian of Eq. (7) no longer has translational symmetry, with energy bands defined only on the average. Further, taking into account the configurational splitting and the vibration-electron

coupling discussed in Sec. II, it is clear that it is not necessary to consider the energy-band structures of solid C_{60} in excessive detail. So we will use the Hubbard Green's function for G_0:

$$G_0(l,l,z) = \frac{2}{(z-E_0) \pm \sqrt{(z-E_0)^2 - B^2}} . \tag{23}$$

Such a function exhibits the correct analytic behavior near the band edges and is frequently used in the problems of excitons.[38,39] The density of states corresponding to the Hubbard Green's function is

$$\rho(E) = \begin{cases} 0 & \text{if } |E-E_0| \geq B \\ \dfrac{2}{\pi B^2}\sqrt{B^2 - (E-E_0)^2} & \text{if } |E-E_0| \leq B. \end{cases} \tag{24}$$

It is seen that E_0 corresponds to $\varepsilon_\alpha - \varepsilon_\beta$, while $2B$ corresponds to the bandwidth of $\varepsilon_{ex}(\mathbf{k})$ which is approximately the sum of the widths of the electron and hole bands.

If $U > B/2$, Eq. (20) has the solution

$$E_B = E_0 - \left(U + \frac{B^2}{4U}\right) \tag{25}$$

and hence

$$b_{B,0} = -\sqrt{1 - \frac{B^2}{4U^2}} . \tag{26}$$

The Hubbard Green's function does not give the explicit formula of $G_0(0,l,z)$, but from the renormalization of $|\psi_{E_B}\rangle$ one gets

$$|b_{B,0}|^2 + \sum_{i \neq 0} |b_{B,i}|^2 = 1 . \tag{27}$$

As discussed in Sec. II, Eq. (21) expresses the relative motion of an e-h pair in a bound state and $|b_{B,0}|^2$ represents the probability of an e-h pair occurring at the same molecule in the excitonic discrete spectrum. $\sum_{i \neq 0} |b_{B,i}|^2 = 1 - |b_{B,0}|^2$ expresses the probability of an e-h pair occurring at different C_{60} molecules. In other words, an exciton in solid C_{60} is a mixed state of $C_{60}{}^*$ and $C_{60}{}^+$-$C_{60}{}^-$. The probability for the occurrence of the former is $|b_{B,0}|^2$ and the total probability for the latter is $1 - |b_{B,0}|^2$. In solid C_{60}, if one takes $B \sim 1$ eV and $U \sim 1.5$ eV, the probability for the occurrence of $C_{60}{}^*$ in the excitonic discrete spectrum is 89%, while the total probability for the state of $C_{60}{}^+$-$C_{60}{}^-$ is only 11%. Figure 2 shows the variation of these probabilities with U/B.

The excitonic continuous spectrum is composed of e-h scattering states (or ionized states of excitons)

$$|\psi_E\rangle = |\mathbf{k}\rangle + G_0^+(E)T^+(E)|\mathbf{k}\rangle , \tag{28}$$

where $|\mathbf{k}\rangle$ is a Bloch state satisfying $\varepsilon_{ex}(\mathbf{k}) = E$. From Eq. (19), one gets
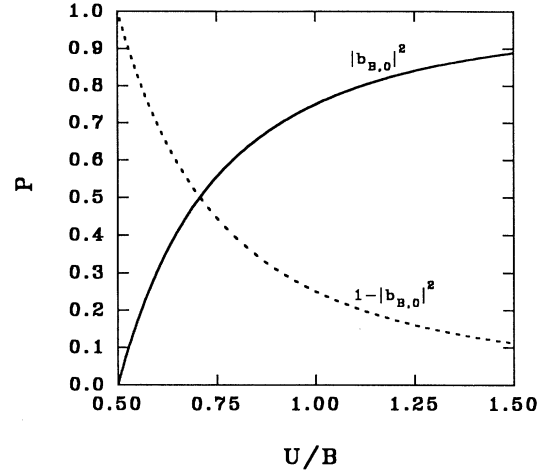

FIG. 2. The variation of probabilities of e-h on the same molecule and different molecules with U/B in an excitonic discrete spectrum, represented by solid and dashed lines, respectively.

$$\langle 0|\psi_E\rangle = \frac{\langle 0|\mathbf{k}\rangle}{1 + UG_0^+(0,0,E)} . \tag{29}$$

In the Koster-Slater model, there is just one bound state of the e-h pair, whose energy is E_B. The range of the continuous spectrum of $\rho(E)$ remains the same as that of $\rho_0(E)$. Hence there exists the sum rule

$$|b_{B,0}|^2 + \int_{-B}^{B} \rho_0(E)|\langle 0|\psi_E\rangle|^2 dE = 1 . \tag{30}$$

With the Hubbard Green's function, one gets

$$|\langle 0|\psi_E\rangle|^2 = \frac{B^2}{B^2 + 4U^2 + 4U(E-E_0)} ,$$

$$f(E) = |\langle 0|\psi_E\rangle|^2 \rho_0(E) = \frac{2}{\pi} \frac{\sqrt{B^2 - (E-E_0)^2}}{B^2 + 4U^2 + 4U(E-E_0)} , \tag{31}$$

where E is in the range $|E-E_0| \leq B$. It is easy to verify that in such a situation Eq. (30) is satisfied.

Excitation of an electron from energy level α to β in the C_{60} molecule will leave a hole in the OMO α and create an electron in the UMO β and will induce several excited states Γ_i, i.e., $\alpha \times \beta = \sum_i \Gamma_i$. Further taking into account the spins of electrons and holes, multiplet structures will form. For example, a hole in the HOMO and an electron in the LUMO couple to form a multiplet structure with T_{1g}, T_{2g}, G_g, and H_g, with singlet and triplet spins. In our theory, we have not taken into account the degeneracies of energy levels and spins of electrons and holes explicitly; hence we have not considered the multiplet structure explicitly. Each multiplet structure of the C_{60} molecule will form a corresponding excitonic multiplet structure in solid C_{60}. Our main purpose here is to reveal the characters of excitons in solid C_{60} and it is not

necessary to consider explicitly the problem of multiplet structure. The results we obtained here are applicable to all the excitonic bands with spins of both singlet and triplet.

V. PHOTOABSORPTIONS IN SOLID C$_{60}$

In the preceding section, a discussion of the discrete and continuous spectra corresponding to interband transitions was given and some concrete calculations were made under a simplifying approximation. The total momentum of optically produced excitons is $\hbar K = \hbar q$, where q is the wave vector of the incident photon. Since $q \approx 0$, we neglect the energy due to the motion of the center of mass. Under such an approximation, the transition probability is proportional to

$$g_0 = n[|b_{B,0}|^2 \delta(\hbar\omega - E_B)$$
$$+ |\langle 0|\psi_E\rangle|^2 \rho_0(E)\delta(\hbar\omega - E)] . \quad (32)$$

Here, n is the number of C$_{60}$ molecules per unit volume. It is assumed that there is just one discrete level. If there exist more than one discrete levels, the first term should be substituted by a sum over those levels. $\rho_0(E)$ is the reduced density of states of e-h bands [the density of states obtained from $\varepsilon_{ex}(k) = \varepsilon_e(k) + \varepsilon_h(-k)$]. Equation (32) clearly indicates that for a particular photoabsorption there is a line spectrum $|b_{B,0}|^2\delta(\hbar\omega - E_B)$, which corresponds to the discrete level of an exciton, and a continuous spectrum $|\langle 0|\psi_E\rangle|^2 \rho_0(E)\delta(\hbar\omega - E) = |\langle 0|\psi_{\hbar\omega}\rangle|^2 \rho_0(\hbar\omega)$, which corresponds to the ionized states of excitons. Due to various effects, there are broadenings in the exciton lines. We may approximately consider that the spectrum-broadening function is the same for different excitonic states, i.e.,

$$f(E - E_0) = \frac{1}{\pi}\frac{\Gamma}{(E - E_0)^2 + \Gamma^2} \quad (33)$$
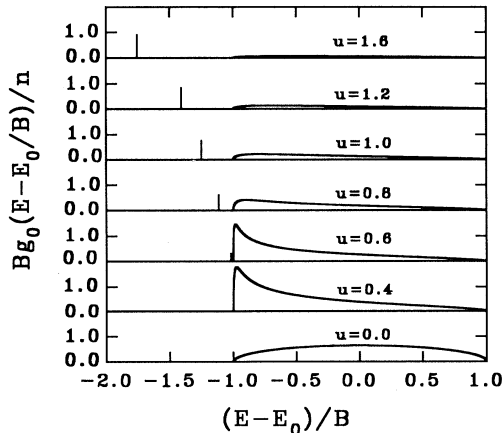
for different E_0's.

FIG. 4. The variation of η with u.

Then the spectra described by Eq. (32) become

$$g = n\left[|b_{B,0}|^2 f(\hbar\omega - E_B)\right.$$
$$\left. + \int f(\hbar\omega - E')|\langle 0|\psi_{E'}\rangle|^2 \rho_0(E')dE'\right] . \quad (34)$$

The normalization condition (30) continues to hold after taking into account the spectrum line broadening.

Figure 3 shows the variations of the absorption spectrum with $u \equiv U/B$, without consideration of the broadenings of spectral lines. It is seen from this figure that when $u = 0$ the absorption spectrum behaves as a peak centered at $\hbar\omega = E_0$ with width $2B$. When u increases gradually, states are pushed towards the lower band edge and at $u = 0.5$ a discrete level is split off the continuum. Further increase of u lowers the energy of the bound level and increases its weight $|b_{B,0}|^2$ at the expense of the continuum; at the same time, the peak of the continuum is shifted to $E_0 - \Delta E_p$, where

$$\Delta E_p = \frac{4B^2}{4U^2 + B^2}U . \quad (35)$$

FIG. 3. The variation of absorption spectrum with $u \equiv U/B$ without considering the broadening of the spectral lines.

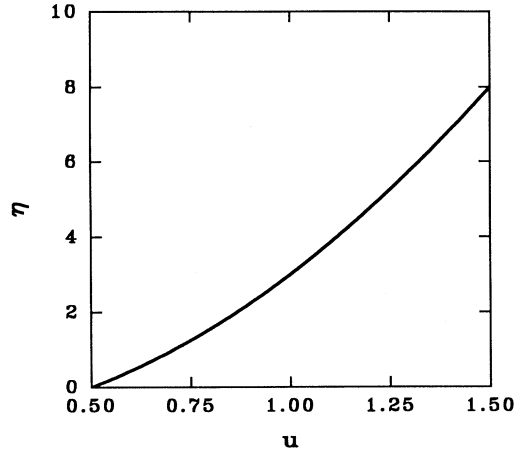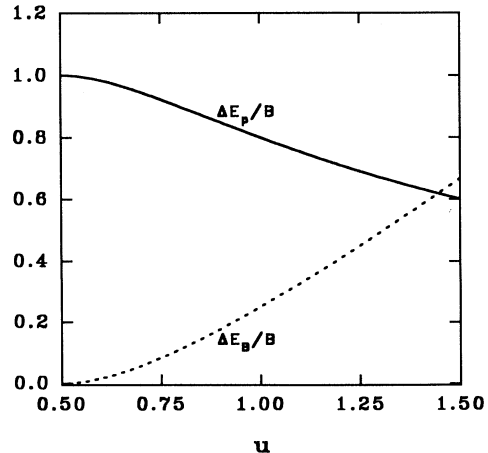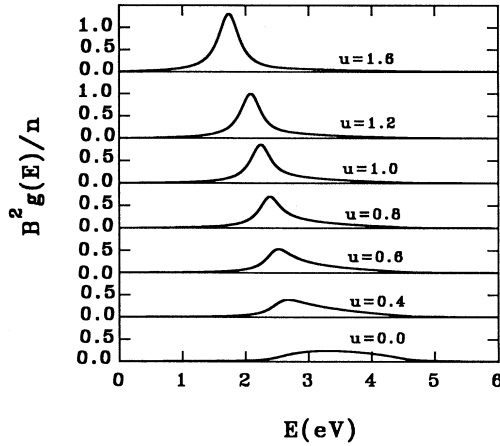FIG. 5. Variations of $\Delta E_p/B$ and $\Delta E_B/B$ vs u.

FIG. 6. Variation of the absorption spectrum with $u \equiv U/B$ after taking into account the broadening of spectral lines.

The ratio between the strength of the discrete level and the total strength of the continuous spectrum (interband absorption) is

$$\eta = \frac{1 - B^2/4U^2}{B^2/4U^2} \ . \tag{36}$$

Figure 4 shows the variations of η with u, while Fig. 5 shows the variations of $\Delta E_p/B$ and $\Delta E_B/B$ with u, where $\Delta E_B = (E_0 - B) - E_B$ is the difference between the discrete level and interband absorption limit. If U/B is taken to be 1.5, we obtain $\eta = 9$, $\Delta E_p/B = 0.6$, and $\Delta E_B/B = 0.67$. In such a case, the strength of the discrete level is dominant and there is an obvious shift in the peak of the continuous spectrum relative to the case of $U/B = 0$. Meanwhile, there is also a clear splitting between the discrete level and the interband absorption limit.

As mentioned above, actual spectral lines should have a broadening. Figure 6 shows the spectrum after taking into account the broadening of the absorption spectral lines. In our calculation, we choose $E_0 = 3.5$ eV, $B = 1$ eV, and $\Gamma = 0.4$ eV. Comparing Fig. 6 with Fig. 3, it is found that the peak in the continuum has been covered by the discrete level and there is just one peak in the absorption spectrum. The interband transitions induce an asymmetry in this peak.

The above discussions refer to dipole-allowed transitions. As for the dipole-forbidden transitions, the crystal field effects and hopping between different molecules will partly allow such transitions. Let us first discuss the crystal field effects concretely. It is well known that the highest symmetry of solid C_{60} is T_h. We can approximately think that the second term in Eq. (7) possesses T_h symmetry, when averaged over the orientations of C_{60} molecules in the crystal lattice. In such a situation, the forbidden $h_u \rightarrow t_{1u}$ transition remains such, while the $g_g \rightarrow t_{1u}$ transition becomes allowed. Results of energy-band calculations indicate that the crystal field splitting is about 0.25 eV.[9] The energy difference between t_{1u} and t_{2u} is about 2 eV. Therefore we can estimate that in the solid the absorption peak due to the $g_g \rightarrow t_{2u}$ transition will be one or two orders of magnitude stronger than that due to the $g_g \rightarrow t_{1u}$ transition. The random parts in the crystal field certainly do not possess inversion symmetry and will permit the $h_u \rightarrow t_{1u}$ transition to become allowed. At present, there is no detailed calculation to estimate this. If we tentatively take it to be ~ 0.1–0.2 eV, then the orientational disorder of the C_{60} molecules will induce some oscillator strength in the $h_u \rightarrow t_{1u}$ transition. But this transition will still be one or two orders of magnitude lower than the $h_u \rightarrow t_{1g}$ transition.

Now let us consider intermolecular hoppings. The matrix element for the discrete excitonic level of the $h_u \rightarrow t_{1g} \rightarrow t_{1u}$ transition is

$$P_{t_{1u},h_u} = - \sum_{i \neq 0} \frac{1}{\varepsilon_{t_{1g}} - \varepsilon_{t_{1u}}} P\lambda_{i,0} b_{B,i} \ , \tag{37}$$

where P is the dipole matrix element of the $h_u \rightarrow t_{1g}$ transition and $\lambda_{i,0}$ is the hopping matrix element between electrons in the t_{1g} state on molecule 0 and the t_{1u} state in molecule i. Obviously, if solid C_{60} possesses T_h point-group symmetry, $\lambda_{i,0}$ will become $\lambda_{-i,0} = -\lambda_{i,0}$ under coordinate inversion $(i \rightarrow -i)$. In Sec. IV we have approximated the excitonic problem with a Koster-Slater model. The wave function of the discrete spectrum of an exciton satisfies $b_{B,i} = b_{B,-i}$. Hence Eq. (37) remains zero in such a situation. Further considering the orientational disorder of the C_{60} molecules, $\lambda_{i,0}$ is also a random quantity, and $\lambda_{i,0} = -\lambda_{-i,0}$ will not hold. It is not difficult to understand that the transition matrix element due to orientational disorder hopping will be larger than that due to randomness in the crystal field. Taking $\lambda_{i,0} \sim 0.5$ eV, $\varepsilon_{t_{1g}} - \varepsilon_{t_{1u}} \sim 1$ eV, it is estimated

TABLE I. Assignment of various optical transitions in the C_{60} molecule and solid C_{60}.

Transitions in C_{60} molecule						Transitions in solid C_{60}				Assignment of transitions
Experimental values (eV)			Theoretical values (eV)			Experimental values (eV)			Theoretical values (eV)	
Ref. 4	Ref. 5	Ref. 6	Ref. 7	Ref. 33	this work	Ref. 1	Ref. 10	Ref. 40	this work	
						1.7	1.7		$\sim$1.8	h_u-t_{1u}
	3.08	3.08	2.9	2.8	2.9	2.73	3.0	2.6	$\sim$2.8	h_u-t_{1g}
3.8	3.79	3.78	3.1	3.1	3.2	3.56	3.7	3.5	$\sim$3.0	h_g-t_{1u}
4.9	4.85	4.83	4.1	4.3	4.2	4.52	4.8	4.4	$\sim$4.2	h_u-h_g
5.97	5.89	5.83			5.4	5.6	5.5	5.5	$\sim$5.3	g_g, h_g-t_{1u}
								5.8		

TABLE II. Parameters used in the calculation of the dielectric function of solid C_{60}. E_i, u_i, and f_i are the central energy, on-site Coulomb attraction between an electron-hole pair, and the oscillator strength for the transition i, respectively.

Transition i	$h_u \rightarrow t_{1g}$	$h_g \rightarrow t_{1u}$	$h_u \rightarrow h_g$	$g_g, h_g \rightarrow t_{2u}$
E_i	3.76	5.01	5.78	6.71
u_i	0.7	1.25	0.96	0.86
f_i	0.52	2.70	7.60	2.70

that for the discrete excitonic line $h_u \rightarrow t_{1u}$ the spectral strength will be one or more orders of magnitude lower than that of the $h_u \rightarrow t_{1g}$ transition. As for the transition to the continuous spectrum, obviously $\langle i|\psi_E \rangle$ is not equal to $\langle -i|\psi_E \rangle$. Therefore, when one does not take into account orientational disorder, the continuous spectrum due to the $h_u \rightarrow t_{1u}$ transition will exist, caused by intermolecular hopping. But the spectral form may greatly change and weaken.

In this paper, we will not discuss higher-order transitions due to interaction between electrons and lattice vibrations. Compared to dipole-allowed transitions, these transitions are rather weak and wide. But if the transitions are forbidden in the C_{60} molecule, it is difficult to say that the transitions induced by the crystal field and intermolecular hopping remain stronger than the vibration-induced transitions.

From the results obtained in the previous sections, we conclude that any transition $\alpha \rightarrow \beta$ in the C_{60} molecule corresponds to an excitonic peak in solid C_{60}. If we take $U \sim 1.5$ eV and $B \sim 1$ eV, it is established that the exciton energy is about 0.1 eV lower than the corresponding molecular excitation. Based on these results, we give an assignment of the optical transitions in the C_{60} molecule and solid C_{60}, as shown in Table I.

In analogy to Wang et al.[1] and Kelly et al.,[40] we choose a set of parameters to calculate the dielectric function of solid C_{60}. In doing so, we only consider those dipole-allowed transitions. In our calculation, we choose $\Gamma = 0.4$ eV and $B = 1.0$ eV for all transitions. The dielectric constant ε_c used to approximate interband absorption well beyond the range of transitions we considered is
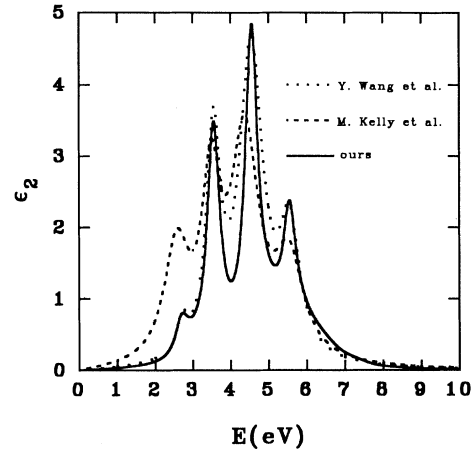

FIG. 7. The imaginary part of the dielectric function of solid C_{60}.

taken to be 2.4. Other parameters are shown in Table II. The imaginary part of the dielectric function is shown in Fig. 7.

VI. CONCLUSIONS

In this paper, we have shown that excitonic effects in solid C_{60} are very important. This can be seen from the quantities η, ΔE_B, and ΔE_p described in Sec. V. It is revealed that excitons in solid C_{60} are intermediate between the Frenkel and Wannier types, although Frenkel characteristics may dominate. Due to the presence of on-site electron-electron Coulomb repulsion (or electron-hole Coulomb attraction), it is required that the single-electron energy-band calculations take this interaction into account. Our work also reveals that photoabsorption in solid C_{60} is largely excitonic. The main peak in the absorption spectrum is due to the transition of a Frenkel type exciton. Photoconductivity in solid C_{60} is probably due to free carrier generation via collisions between excitons and defects or surfaces, or via exciton-exciton collisions.

[1] Y. Wang, J. M. Holden, A. M. Rao, W. T. Lee, X. X. Bi, S. L. Ren, G. W. Lehman, G. T. Hager, and P. C. Eklund, Phys. Rev. B **45**, 14396 (1992).

[2] A. Skumanich, Chem. Phys. Lett. **182**, 486 (1991).

[3] J. Mort, K. Okumura, M. Machonkin, R. Ziolo, D. R. Huffman, and M. I. Ferguson, Chem. Phys. Lett. **186**, 281 (1991).

[4] H. Ajie, M. M. Alvarez, S. J. Anz, R. D. Beck, F. Diederich, F. Fostiropoulos, D. R. Huffman, W. Krätschmer, Y. Rubin, K. E. Schriver, D. Sensharma, and R. L. Whetten, J. Phys. Chem. **94**, 8639 (1990).

[5] J. P. Hare, H. W. Kroto, and R. Taylor, Chem. Phys. Lett. **177**, 394 (1991).

[6] Z. Gasyna, P. N. Schatz, J. P. Hare, T. J. Dennis, H. W. Kroto, R. Taylor, and D. R. M. Walton, Chem. Phys. Lett. **183**, 283 (1991).

[7] S. Saito and A. Oshiyama, Phys. Rev. Lett. **66**, 2637 (1991).

[8] W. Y. Ching, M. Z. Huang, Y. N. Xu, W. G. Harter, and F. T. Chen, Phys. Rev. Lett. **67**, 2045 (1991).

[9] N. Troullier and J. L. Martins, Phys. Rev. B **46**, 1754 (1992).

[10] G. Gensterblum, J. J. Pireaux, P. A. Thiry, R. Caudano, J. P. Vigneron, Ph. Lambin, A. A. Lucas, and W. Krätschmer, Phys. Rev. Lett. **67**, 2171 (1991).

[11] C. Reber, L. Yee, J. Mckiernan, J. I. Fink, R. S. Williams, W. M. Tong, D. A. A. Ohlberg, R. L. Whetten, and F. Dierderich, J. Phys. Chem. **95**, 2127 (1991).

[12] M. B. Matus, H. Kuzmany, and E. Sohmen, Phys. Rev. Lett. **68**, 2822 (1992).

[13] R. W. Lof, M. A. Van Veenendaal, B. Koopmans, H. T. Jonkman, and G. A. Sawatzky, Phys. Rev. Lett. **68**, 3924 (1992).

[14] M. K. Nissen, S. M. Wilson, and M. L. W. Thewalt, Phys. Rev. Lett. **69**, 2423 (1992).

[15] L. Resca, Phys. Rev. Lett. **71**, 2839 (1993).

[16] P. J. Benning, J. L. Martins, J. H. Weaver, L. P. F. Chibante, and R. E. Smalley, Science **252**, 1417 (1991).

[17] J. H. Weaver, J. Phys. Chem. Solids **53**, 1433 (1992).

[18] T. Takahashi, S. Suzuki, T. Morikawa, H. Katayama-Yoshida, S. Hasegawa, H. Inokuchi, K. Seki, K. Kikuchi, K. Ikemoto, and Y. Achiba, Phys. Rev. Lett. **68**, 1232 (1992).

[19] E. L. Shirley and S. G. Louie, Phys. Rev. Lett. **71**, 133 (1993).

[20] M. S. Hybersten and S. G. Louie, Phys. Rev. Lett. **55**, 1418 (1985); Phys. Rev. B **32**, 7005 (1985); **34**, 5390 (1986).

[21] A. S. Davydov, *Theory of Molecular Excitons* (Plenum, New York, 1971).

[22] For example, see R. C. Haddon, L. E. Brus, and K. Raghavachari, Chem. Phys. Lett. **125**, 459 (1986); S. Satpathy, *ibid.* **130**, 545 (1986); O. Gunnarsson, S. Satpathy, O. Jepsen, and O. K. Anderson, Phys. Rev. Lett. **67**, 3002 (1991); V. de Coulon, J. L. Martins, and F. Reuse, Phys. Rev. B **45**, 13 671 (1992).

[23] For instance, W. A. Harrison, Phys. Rev. **118**, 1182 (1960); J. C. Phillips, *ibid.* **125**, 1931 (1962); J. Callaway, *Energy Band Theory* (Academic Press, New York, 1964); M. L. Cohen and T. K. Bergstresser, Phys. Rev. **141**, 789 (1966); M. L. Cohen and V. Heine, in *Solid State Physics: Advances in Research and Applications*, edited by H. Ehrenreich *et al.* (Academic Press, New York, 1970), Vol. 24, p. 138; M. L. Cohen, Phys. Today **33** (7), 40 (1979).

[24] Xu-Dong Jiang and Zi-Zhao Gan (unpublished).

[25] V. P. Antropov, O. Gunnarsson, and O. Jepsen, Phys. Rev. B **46**, 13 647 (1992).

[26] R. L. Martin and J. P. Ritchie, Phys. Rev. B **48**, 4845 (1993).

[27] G. A. Gallup, Chem. Phys. Lett. **187**, 187 (1991).

[28] R. Saito, G. Dresselhaus, and M. S. Dresselhaus, Phys. Rev. B **46**, 9906 (1992).

[29] W. G. Harter and D. E. Weeks, J. Chem. Phys. **90**, 4727 (1989); **90**, 4744 (1989).

[30] M. Lannoo, G. A. Baraff, M. Schlüter, and D. Tománek, Phys. Rev. B **44**, 12 106 (1991); M. Schlüter, M. Lannoo, M. Needels, G. A. Baraff, and D. Tománek, Phys. Rev. Lett. **68**, 526 (1992); V. de Coulon, J. L. Martins, and F. Reuse, Phys. Rev. B **45**, 13 671 (1992); R. D. Bendale, J. F. Stanton, and M. C. Zerner, Chem. Phys. Lett. **194**, 467 (1992).

[31] F. Negri, G. Orlandi, and F. Zerbetto, Chem. Phys. Lett. **144**, 31 (1988); J. Chem. Phys. **97**, 6496 (1991).

[32] K. Yabana and G. F. Bertsch, Chem. Phys. Lett. **197**, 32 (1992).

[33] P. A. Brühwiler, A. J. Maxwell, A. Nilsson, N. Mårtenson, and O. Gunnarsson, Phys. Rev. B **48**, 18 296 (1993).

[34] A. F. Hebard, R. C. Haddon, R. M. Fleming, and A. R. Kortan, Appl. Phys. Lett. **59**, 2109 (1991).

[35] J. C. Slater and G. F. Koster, Phys. Rev. **94**, 1498 (1954).

[36] E. N. Economou, *Green's Functions in Quantum Physics* (Springer, Berlin, 1990).

[37] P. A. Heiney, J. E. Fischer, A. R. McGhie, W. J. Romanow, A. M. Denenstein, J. P. McCauley, Jr., A. B. Smith III, and D. E. Cox, Phys. Rev. Lett. **66**, 2911 (1991); R. Sachidanandam and A. B. Harris, *ibid.* **67**, 1467 (1991); R. Tycko, G. Dabbagh, R. M. Fleming, R. C. Haddon, A. V. Makhija, and S. M. Zahurak, *ibid.* **67**, 1886 (1991).

[38] D. K. G. de Boer, C. Haas, and G. A. Sawatzky, Phys. Rev. B **29**, 4401 (1984).

[39] V. L. Broude, E. I. Rashba, and E. F. Sheda, *Spectroscopy of Molecular Excitons* (Springer-Verlag, Berlin, 1985).

[40] M. K. Kelly, P. Etchegoin, D. Fuchs, W. Krätschmer, and K. Fostiropoulos, Phys. Rev. B **46**, 4963 (1992).